Tellus (1997), 49B, 556–565
Printed in UK – all rights reserved

TELLUS
ISSN 0280–6509

NO_x during ozone depletion events in the arctic troposphere at Ny-Ålesund, Svalbard

By HARALD J. BEINE[1, 2]*, DANIEL A. JAFFE[1], FRODE STORDAL[2], MAGNUZ ENGARDT[3], SVERRE SOLBERG[2], NORBERT SCHMIDBAUER[2] and KIM HOLMÉN[3] [1]*Geophysical Institute and Department of Chemistry, University of Alaska, 903 N. Koyukuk Dr., Fairbanks, Alaska 99775–7320, USA,* [2]*Norwegian Institute for Air Research (NILU), Instituttveien 18, N-2007 Kjeller, Norway,* [3]*Department of Meteorology, Stockholm University (MISU), S-106 91 Stockholm, Sweden*

(Manuscript received 22 May 1996; in final form 13 June 1997)

ABSTRACT

Measurements of NO_x, ozone, non-methane hydrocarbons (NMHC), and other atmospheric constituents were made at the Zeppelin-mountain atmospheric monitoring station near Ny-Ålesund, Svalbard, during the spring of 1994. On a few occasions, we observed tropospheric ozone depletion events with minimum ozone mixing ratios of 3.9 ppbv that lasted for up to 2 days. This paper presents the first measurements of NO_x during ozone depletion events. The objective of this work is to explore the role of NO_x during those periods. During depletion periods, mixing ratios of NO_x, total NMHC, and acetylene dropped to minima of <4.5 pptv, 3.6 ppbCv, and 123 pptv, respectively. These mixing ratios were significantly lower than the means for our campaign, which were 23.6 pptv, 14.3 ppbCv, and 478 pptv, respectively. Because NO_2 would quickly scavenge the BrO radical, the low observed NO_x mixing ratios are consistent with proposed mechanisms involving catalytic destruction of ozone by the Br radical. A mechanism involving NO_x to recycle halogen radicals seems unlikely in light of the current study.

1. Introduction

The depletion of tropospheric ozone is frequently observed in the arctic maritime boundary layer during the winter-spring transition (Hopper et al., 1994). While measurements at Alert, NWT (Barrie et al., 1988; Bottenheim et al., 1990; Barrie et al., 1994), at Ny-Ålesund, Svalbard (Solberg et al., 1996a) and at Barrow, Alaska (Sturges et al., 1993) have revealed many interesting results regarding aerosol and radical chemistry, no reliable measurements of NO_x ($NO+NO_2$) have been reported for these events. The objective of this work is to present and explore NO_x measurements taken during ozone depletion events at Ny-Ålesund, Svalbard during the spring of 1994.

Central to the current understanding of the ozone depletion mechanism in the arctic troposphere is the catalytic cycling of Br atoms (Barrie et al., 1988; Bottenheim et al., 1990; Finlayson-Pitts et al., 1990; McConnell et al., 1992; Fan and Jacob, 1992). So far, five different mechanisms have been proposed by different authors for the production and recycling of bromine species during ozone depletion processes. Hausmann and Platt (1994) have recently summarized the various mechanisms. The key steps in tropospheric ozone destruction are:

$$Br + O_3 \rightarrow BrO + O_2 \quad (1)$$

$$2BrO \rightarrow Br_2 + O_2 \quad (2)$$

$$Br_2 \xrightarrow{h\upsilon} 2Br \quad (3)$$

* Corresponding author.

Tropospheric NO_x is photochemically oxidized to HNO_3, PAN, or other NO_y ($=NO_x+PAN+HNO_3+N_2O_5+RNO_2+\ldots$) species. NO_x in the troposphere governs in-situ ozone production.

$$NO+O_3\rightarrow NO_2+O_2 \quad (4)$$

$$NO_2 \xrightarrow{h\upsilon} NO+O \quad (5)$$

$$O_2+O\rightarrow O_3 \quad (6)$$

$$NO+RO_2\rightarrow NO_2+RO \quad (7)$$

The ultimate sink for NO_x is nitric acid HNO_3, which is dry or wet deposited.

$$NO_2+OH\rightarrow HNO_3 \quad (8)$$

A number of possible interactions between NO_x and halogen radicals during ozone depletion were formulated by various authors. NO_x can return BrO to Br (Barrie et al., 1988). Reaction 9 forms together with reactions 1, 4, and 5 a null cycle which limits ozone destruction.

$$BrO+NO\rightarrow Br+NO_2 \quad (9)$$

Additionally, NO_2 would be scavenged by BrO to form $BrONO_2$ (reaction 10), which could be returned to the reactants by photolysis, or hydrolyzed to produce nitric acid (Fan and Jacob, 1992). The presence of ice crystals would enhance this scavenging process (Curry and Radke, 1993).

$$BrO+NO_2\rightarrow BrONO_2 \quad (10)$$

$$BrONO_2+H_2O\rightarrow HOBr+HNO_3 \quad (11)$$

Alternatively, NO_x was proposed to be important in the initial formation of bromine radicals; BrNO or $BrNO_2$ may be produced from NO_2 or N_2O_5 and NaBr, contained in sea-salt aerosols. Subsequent photolysis releases the Br radical (Sturges, 1989; Finlayson-Pitts et al., 1990):

$$2NO_2(g)+NaBr(s)\rightarrow BrNO(g)+NaNO_3(s) \quad (12)$$

$$N_2O_5(g)+NaBr(s)\rightarrow BrNO_2(g)+NaNO_3(s) \quad (13)$$

$$BrNO \xrightarrow{h\upsilon} Br+NO \quad (14)$$

$$BrNO_2 \xrightarrow{h\upsilon} Br+NO_2 \quad (15)$$

The presence of NO_x in a tropospheric airmass above a certain mixing ratio promotes the formation of ozone (Lin et al., 1988; Liu et al., 1987). The simultaneous presence of high mixing ratios of Br-species and NO_x is unlikely from the above reactions; NO is quickly converted to NO_2, and NO_2 subsequently depleted. The presence of NO_x ties BrO and slows down ozone depletion (Barrie, 1988). Model calculations have shown that NO_x is quickly lost during ozone depletion events (McConnel et al., 1992; Fan and Jacob, 1992).

Our measurements of NO_x and other atmospheric constituents (Beine et al., 1996; 1997) were not focused on ozone depletion, but on the understanding of the sources of NO_x in the arctic troposphere and its influence on the ozone budget. In this paper we explore the NO_x behavior during the few ozone depletion events that occurred during the campaign, and discuss the consistency of our findings with possible mechanisms of ozone depletion.

2. Experiment

Measurements of NO_x were performed from 19 February to 31 May 1994 at the atmospheric monitoring station of the Norwegian Institute for Air Research (NILU) at the Zeppelin mountain near Ny-Ålesund, Svalbard (78°54′42″ N, 11°53′30″ E.), 474 m a.m.s.l. The station is part of the Ny-Ålesund International Arctic Research and Monitoring Facility. Ozone, NMHCs, and aerosol particles are measured at the same location routinely throughout the year by NILU and the Meteorological Department, Stockholm University (MISU), respectively. The detailed procedures for NO_x, ozone, and the nephelometer are described in Beine et al. (1996; 1997). The measurements of NMHCs are described by Solberg et al. (1996 a,b, and references therein). Thus only a short overview is given here; Ozone was measured using a UV-absorption ozone analyzer (Monitor Labs model 8810), NO was measured using a high-sensitivity chemiluminescence detector, NO_2 was detected as NO following broad-band photodissociation (Kley and McFarland, 1980) by a 300 W Xe-arc lamp. The NO_x ($NO+NO_2$) 3σ detection limit was 4.5 pptv in a 1-h average (6, 1-min samples each for NO and NO_2). In this paper NO_x data below the detection limit are reported with their numerical value and used to calculate

statistical parameters. More information about the accuracy and precision of the NO_x instrument can be found in Beine et al. (1997). Accumulation mode particles were measured using a nephelometer (developed at MISU). NMHC canister samples were taken daily and later analyzed by GC-FID (Chrompack VOC-AIR). 3-dimensional back trajectories were calculated using the Irish Meteorological Service trajectory model (McGrath, 1989). Trajectories were calculated for depletion events 4 times a day. They arrive at 950 hPa and extend for 3 days backwards in time. The trajectories are calculated from the initialized analysis at the European Center for Medium Range Weather Forecast (ECMWF).

Data reported here are one-minute or hourly averages except NMHC, which were collected once daily. Data are reported in day of year (DOY), whereby January 1 = DOY 1. Times are reported in local time (LT), where LT = UT + 1.

3. Results

Table 1 presents a statistical overview of the observed background mixing ratios of ozone, acetylene, and NO_x for the entire campaign. Acetylene is shown because it is most affected during ozone depletion events (Jobson et al., 1994; Solberg et al., 1996a). More detailed information regarding the influence of different airmasses can be found in Beine et al. (1996). The photochemistry during this period is discussed by Beine et al. (1997).

Fig. 1 shows the timeseries for ozone, acetylene, and NO_x during our campaign. To identify periods of ozone depletion two criteria were used: All periods where ozone mixing ratios fell below 25 ppbv were flagged. This mixing ratio was considered a lower limit for background ozone levels, not influenced by ozone depletion (Solberg et al., 1996a). 189 hourly averages on 19 different days were below 25 ppbv. Of those data only periods with a median ozone mixing ratio below 20 ppbv were considered "ozone depleted". These low ozone data appeared in 4 periods that lasted up to two days. Since statistical values such as mean and medians vary with the somewhat arbitrary selection process for the episodes we include in Table 2 the minimum mixing ratios for ozone and NO_x found during each event together with the medians.

The available NMHC data during the low ozone events are rather sparse, since canister samples were taken only once daily, and the sampling times were not coordinated to search for ozone depletion events. Only a total of 6 NMHC samples were taken during ozone depletion. Most affected during ozone depletion is acetylene, which is shown in Fig. 1. A comparison of the NMHC mixing ratios during the events with non-ozone depletion behavior is difficult from this set in a statistical meaningful way, since the NMHC mixing ratios showed a significant decreasing trend during the campaign. NMHC mixing ratios during ozone depletion events at Zeppelin are discussed in detail by Solberg et al. (1996a).

The ozone depletion events identified above showed the same general features, which have been identified before for the Zeppelin station (Solberg et al., 1996a), and other locations (Anlauf et al., 1994; Hopper and Hart, 1994; Jobson et al., 1994; Staebler et al., 1994; Sturges et al., 1993). As an example we show events 2 and 3 in Fig. 2. These two events were close together in time, and the ozone mixing ratio did not recover to the median value of 39 ppbv in between. The intermittent period did not meet the criterion of ozone being below 25 ppbv. Nevertheless, it showed indication of depletion, and probably reflected

Table 1. *Statistical overview of the background data during spring 1994*

	O_3 (ppbv) $n = 2110$ h	Acetylene (pptv) $n = 56$ samples	NO_x (pptv) $n = 1811$ h
mean	35.5	478.0	23.6
SD	8.6	27.9	14.5
minimum	3.9	123.0	0.0
maximum	49.5	939.0	143.9
median	37.2	477.4	21.5

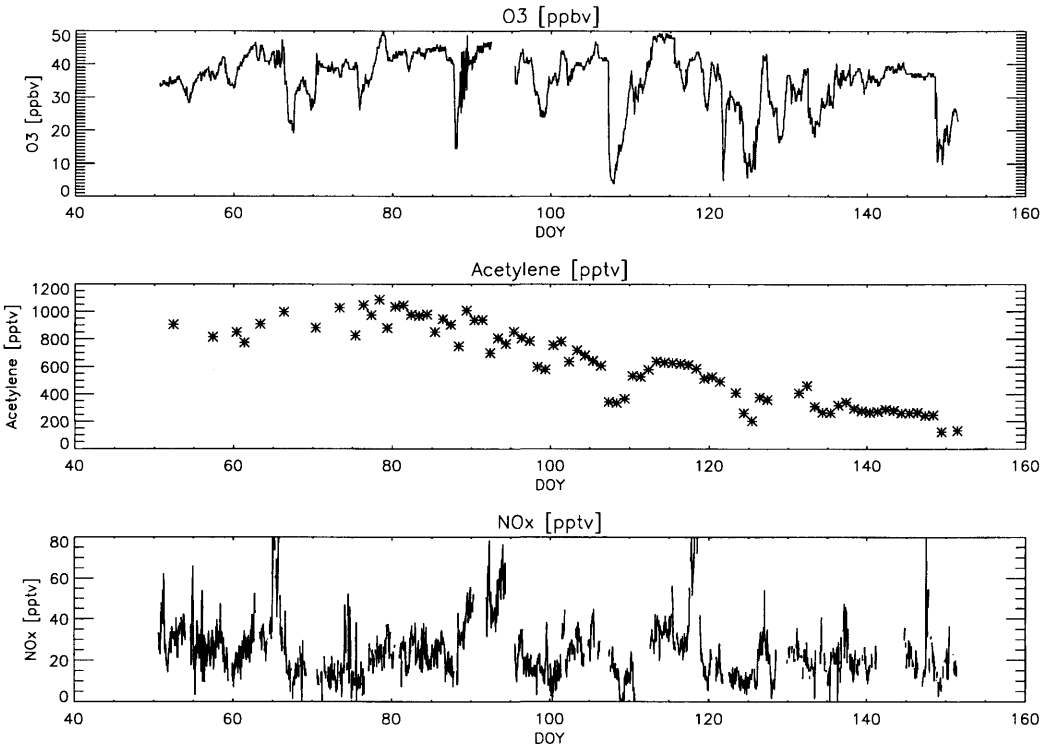

Fig. 1. Timeseries of ozone [ppbv], acetylene [pptv], and NOx [pptv] at Zeppelin during spring 1994 (DOY 51–151).

Table 2. *Ozone depletion events*

Event	Start	End	n (h)	Median O_3 (ppbv)	Min O_3 (ppbv)	Median NO_x (pptv)	Min NO_x (pptv)
1	107.45	109.54	48	13.6	3.9	12.1	0 (below d.l.[a])
2	121.54	121.79	7	12.2	4.7	12.8	8.8
3	124.0	126.20	48	12.6	5.6	9.3	3.5 (below d.l.)
4	148.54	150.5	36	16.6	9.7	11.7	2.5 (below d.l.)

[a] d.l. $= 3\sigma$ detection limit.

mixing with non-depleted air. In the following we will discuss them together as one depletion period. Fig. 2 shows the timeseries for ozone, wind direction, temperature, σ_{sp}, and NO_x.

Days 121 to 126 were meteorologically homogeneous, with cold, clean air coming from the north, as indicated by the trajectories, which are shown in Fig. 3 for the entire period (DOY 120 — DOY 128). The onset of low ozone events was connected to a shift in the local wind direction to north-westerly directions after the passage of a cold front. Temperature was lower than average throughout the depletion period, the average temperature at Ny-Ålesund is -3.5°C at the beginning of May (Hansen-Bauer et al., 1990). Anticorrelated to the ozone drop, the scattering coefficient rose from 4 up to 6 (10^{-6} m^{-1}) on DOY 124. Following the first drop in the ozone mixing ratio, the NO_x mixing ratio decreased to low levels for 4 days. The measured NO_x mixing ratios were around 10 pptv. NO mixing ratios were at or below the detection limit (1.6 pptv) and showed no diurnal

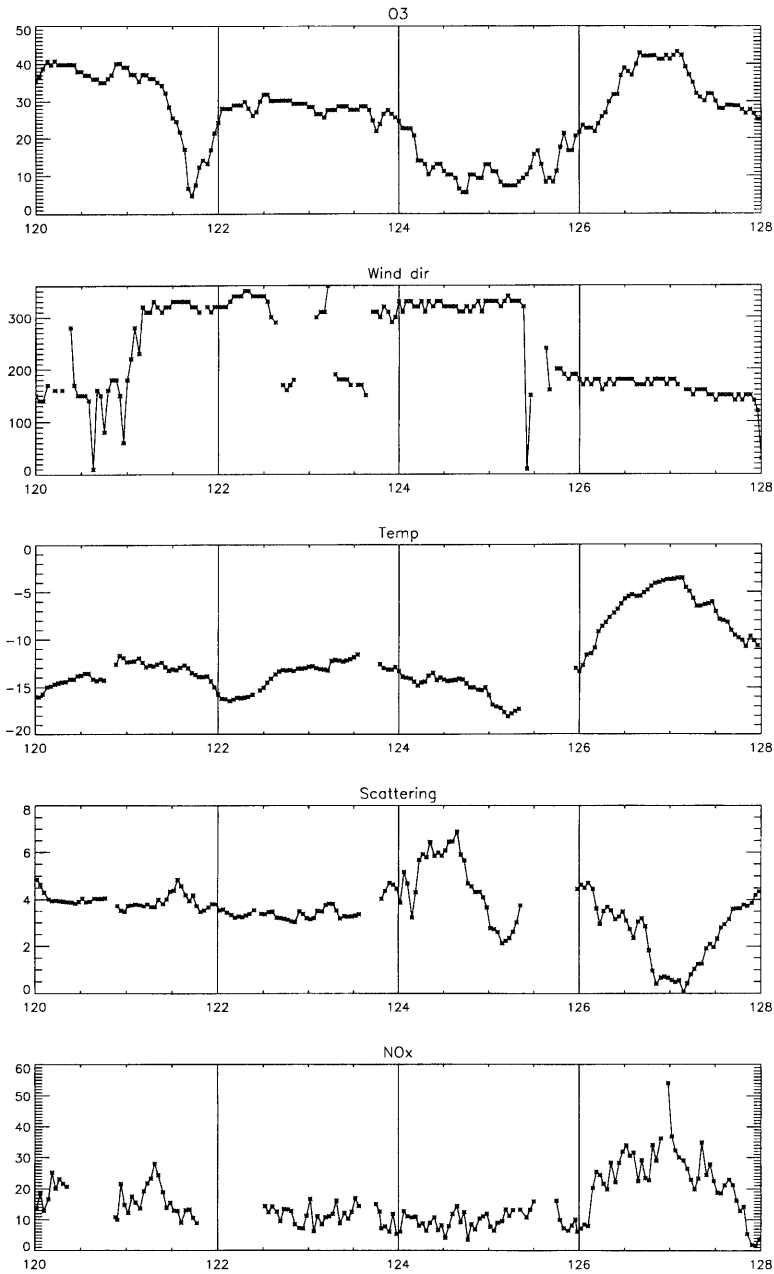

Fig. 2. Ozone depletion events 2 and 3: Timeseries of ozone [ppbv], wind direction [°], temperature [°C], scattering coefficient σ_{sp} ($10^{-6}m^{-1}$), and NO_x (pptv) during DOY 120–128, 1994.

cycle. Consequently the NO/NO_2 ratio cannot be accurately determined.

Ozone depletion events at Alert during PSE 1992 were connected to a capping inversion at a height of 300–400 m (Anlauf et al., 1994), capping inversions were also observed at Ny-Ålesund during ozone depletion periods (Solberg et al., 1996a). Radiosoundings show that low ozone

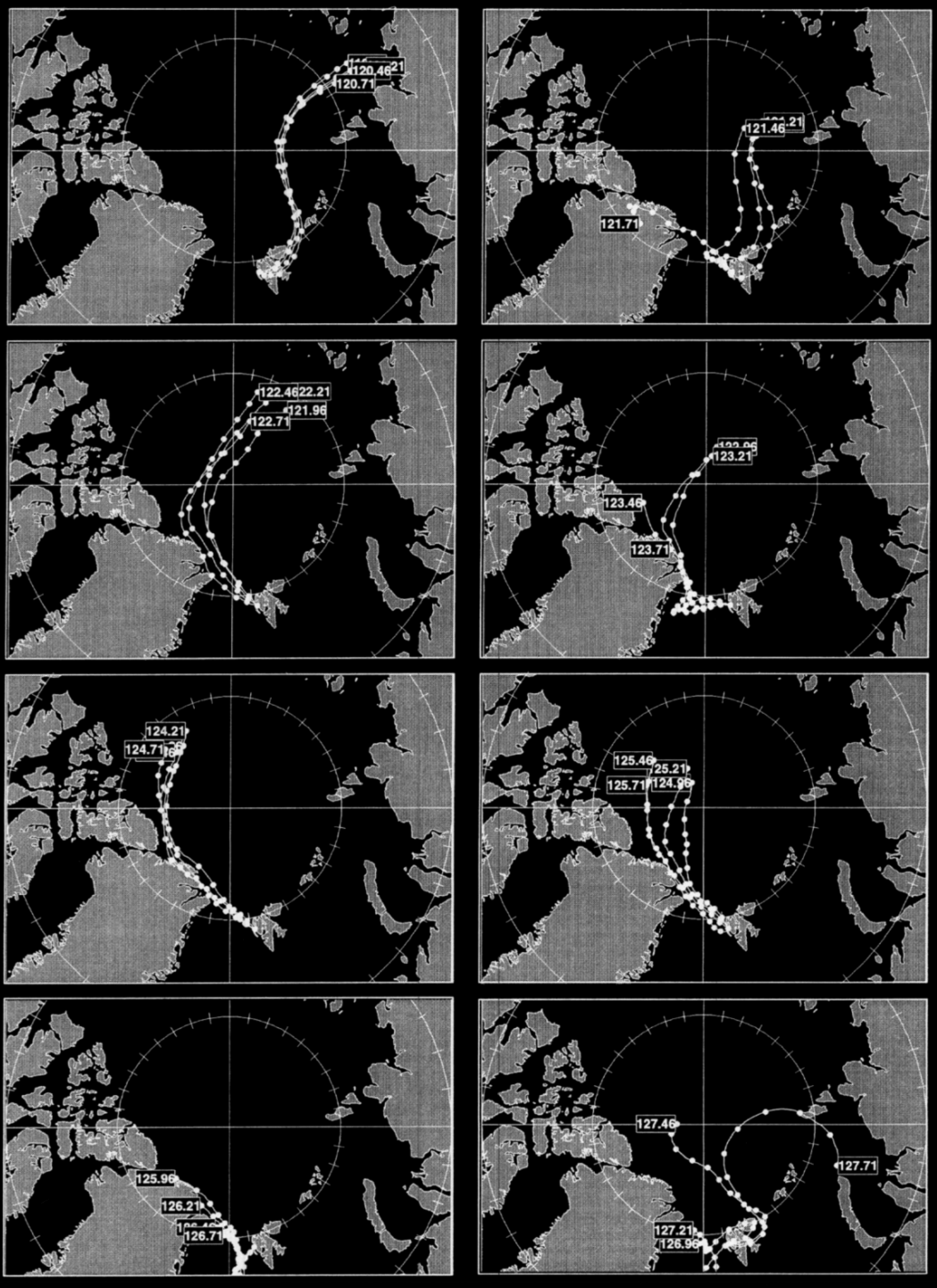

Fig. 3. 3-day, 3-dimensional back trajectory for DOY 121 — DOY 128 arriving at Zeppelin. The dots mark 6 h in time. The boxes at the end indicate the arrival time at Zeppelin in LT.

mixing ratios were found in a mixed layer that can extend up to about 1000 m. Fig. 4 shows the potential temperature and the ozone mixing ratio measured by radio sondes for four days, DOY 121, 122, 125, and 126, launched at 12:00 UT at sea level at Ny-Ålesund. On DOY 121 and 125 a layer of low stability extended to about 530 m altitude, only 60 m above the station. Ozone mixing ratios in this layer varied from 13 to 17 ppbv, with the onset of the inversion ozone mixing ratios returned to values around 50 ppbv within 500 m. The capping inversion was higher on DOY 122 and 123, consistent with the higher ozone mixing ratios found on these days. It then dropped during the remainder of the ozone depletion event. At the onset of day 126 mixing ratios of ozone and NO_x were increasing, while the scattering coefficient dropped to very low values. The radiosounding on day 126 showed a stratified lower troposphere and a fairly uniform ozone gradient of about 6 ppbv/km throughout the lower troposphere. This marked the end of the low ozone episode.

Three-dimensional back trajectories (Fig. 3) show for this period that ozone depletion occurred most strongly when the air mass passed the north-east coast of Greenland about 1.5 days prior to arrival at Ny-Ålesund at altitudes below a few hundred meters. The first short ozone depletion event on DOY 121 was connected with a short change in the flow to north-westerly directions. On DOY 122 and 123, when ozone mixing ratios returned to around 30 ppbv, the airmass arrived from a more northerly direction, and did not pass the northern coast line of Greenland any more. In addition, a weak cyclone passed Svalbard on DOY 123. Finally on DOY 126, the trajectory arrived from the open waters of the Greenland sea when ozone returned to normal mixing ratios and the scattering coefficient dropped to low values.

Analysis of meteorology and trajectories at Alert showed that ozone depletion events were con-

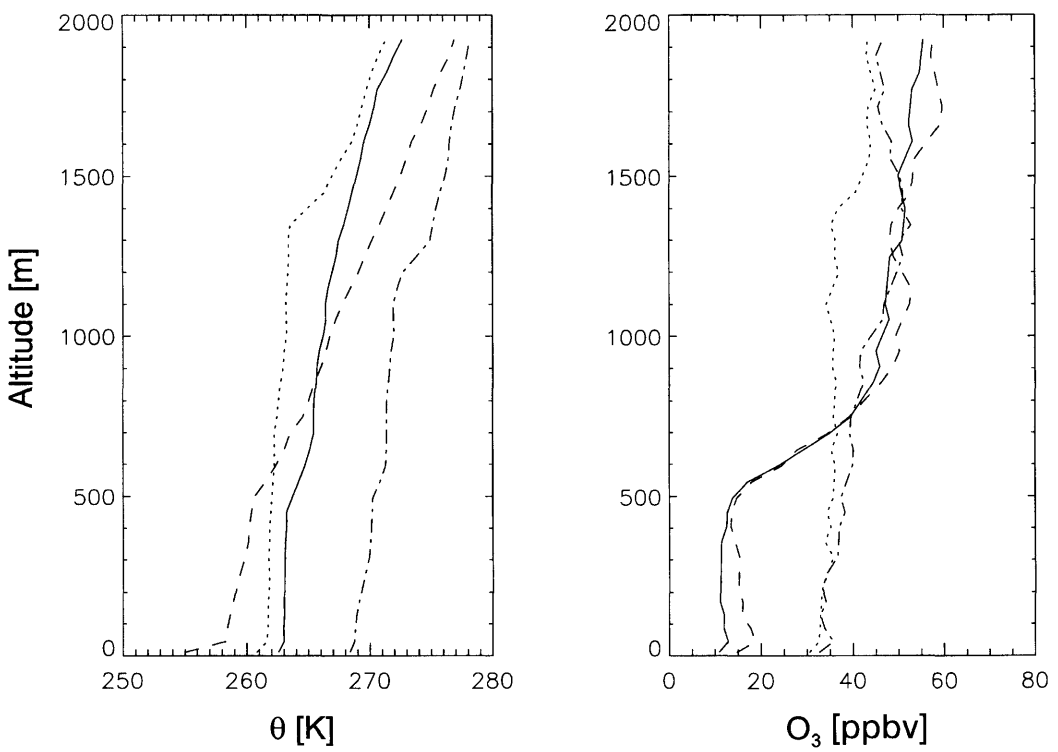

Fig. 4. Ozone sounding for DOY 121 (solid line), 122 (dotted line), 125 (dashed line), and 126 (dash-dot line) (12:00 UT). The left panel shows potential temperature Θ [K], the right panel shows ozone mixing ratios (ppbv).

nected to north/north-easterly flow (Bottenheim et al., 1990; Hopper and Hart, 1994). Results from an ice camp off the coast of Alert, however, showed that air during ozone depletion events originated from close proximity to the surface of the Arctic ocean, but showed no significant correlation with any source region (Hopper et al., 1994). Sturges et al. (1993) showed that ozone depletion at Barrow, Alaska was connected to air transport over areas of open water in the otherwise frozen Arctic Ocean.

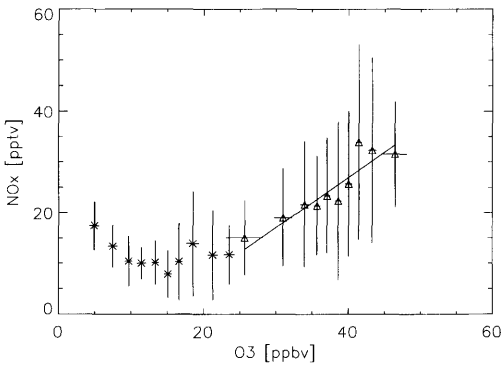

Fig. 5. Scatterplot of ozone versus NO_x. Stars show periods of ozone depletion (as defined in the text), triangles show all other ozone data. For the 2 groups, the data were sorted and grouped into 10th percentiles by the ozone mixing ratio. The line for the non-depleted ozone data shows Theil's non-parametric regression, the slope is 0.99 (pptv NO_x/ppbv O_3).

4. Discussion of observed NO_{ix}

NO_x during the observed ozone depletion events was in general low, about 10 pptv below the overall median of the entire campaign. The two species did not always show similar trends concurrently during low ozone episodes, for example during event #1 (DOY 107.5–109.5), low NO_x seemed to lag behind low ozone by up to one day, while during event #4 (DOY 148.5–150.5) a correlated reduction in both NO_x and ozone was seen.

Table 3 shows statistics of the NO_x mixing ratios for all of the low ozone periods. This statistics was derived from the measured 1-min averages and thus shows more scatter than in Fig. 1. No diurnal cycles of NO_x or the NO/NO_2 ratio were observed. NO_x showed a median value of 11.8 pptv, which was about half than during all other periods.

In Fig. 5, a scatterplot of NO_x versus ozone is shown. The data are sorted and grouped into 10th percentiles by the ozone mixing ratio for ozone depletion periods as defined above and all other ozone data. The line for the latter category is calculated using Theil's nonparametric regression (Miller and Miller, 1984), the slope is 0.99 (pptv NO_x/ppbv O3). The behavior of NO_x during the low ozone events was not as uniform. Above about 10 ppbv ozone, no correlation with NO_x was seen, below this value NO_x and ozone appeared to be anticorrelated. This might be due to the fact that the onset of low NO_x lagged behind the onset of low ozone during some of the periods. Thus, NO_x reached a minimum when the ozone mixing ratio was stable or recovering. However, our data do not give sufficient statistical basis for a further discussion of general trends.

The observation of very low NO_x mixing ratios is consistent with the discussed mechanism above, both NO and NO_2 can be removed by reaction with BrO. Thus the absence of NO_x makes ozone depletion more efficient. A mechanism involving NO_x to recycle Br radicals seems unlikely. Rather, the low observed NO_x suggests that the recycling of BrO to Br occurs via other channels, such as reaction with BrO or ClO (Le Bras and Platt, 1995), or heterogeneous reactions (McConnell et al., 1992; Fan and Jacob, 1992; Abbatt, 1994).

Table 3. *Statistics of NO_x*

	NO_x (ozone depletion)	NO_x (all other data)
n (min)	932	10842
mean (pptv)	14.3	28.2
SD (pptv)	26.8	40.3
Median (pptv)	11.8	23.9

5. Conclusion

During 4 ozone depletion periods at the Zeppelin station on Svalbard very low NO_x mixing ratios were observed. The minimum ozone and NO_x mixing ratios were 3.9 ppbv and below the detection limit of 4.5 pptv, respectively. The absence of NO_x is consistent with mechanisms involving halogen chemistry to destroy ozone. Furthermore it supports mechanisms that do not involve NO_x to recycle those halogens. However, in order to fully understand the role of NO_x, several depletion events in varying stages have to be observed with a more sensitive instrument in a future campaign. To quantify the observations, detection limits of less than 1 pptv and around 1 pptv are necessary for NO and NO_2, respectively, in a 1-min average.

6. Acknowledgements

We thank the Alfred Wegener Institut for making the ozone soundings available, and Ray McGrath at ECMWF for providing access to his trajectory model. The support of NILU's NADIR database is acknowledged. Funding for this work was provided by NSF (grant # ATM-9215127) to the Geophysical Institute, University of Alaska, and the Norwegian Research Council and EC (contract EV5V-CT93–0318) to NILU. The MISU monitoring activities are financed by the Swedish Environmental Protection Agency.

REFERENCES

Abbatt, J. P. D. 1994. Heterogeneous reaction of HOBr with HBr and HCl on ice surfaces at 228 K. *Geophys. Res. Lett.* **21**, 665–668.

Anlauf, K. G., Mickle, R. E. and Trivett, N. B. A. 1994. Measurements of ozone during Polar Sunrise Experiment 1992. *J. Geophys. Res.* **99**, 25, 345–25, 354.

Barrie, L. A., Bottenheim, J. W., Schnell, R. C., Crutzen, P. J. and Rasmussen, R. A. 1988. Ozone destruction and photochemical reactions at polar sunrise in the lower arctic atmosphere. *Nature* **334**, 138–141.

Barrie, L. A., Bottenheim, J. W. and Hart, W. R. 1994. Polar Sunrise Experiment 1992 (PSE 1992): Preface. *J. Geophys. Res.*, **99**, 25, 313–25, 314.

Barrie, L. A., Li, S.-M., Toom, D. L., Landsberger, S. and Sturges, W. T. 1994. Lower tropospheric measurements of halogens, nitrates, and sulphur oxides during Polar Sunrise Experiment 1992. *J. Geophys. Res.* **99**, 25, 453–25, 468.

Beine, H. J., Engardt, M., Jaffe, D. A., Hov, Ø., Holmén, K. and Stordal, F. 1996. Measurements of NO_x and aerosol particles at the Ny-Ålesund Zeppelin mountain-station on Svalbard: Influence of local and regional pollution sources. *Atmos. Environ.* **30**, 1067–1079.

Beine, H. J., Jaffe, D. A., Herring, J. A., Kelley, J. A. Krognes, T. and Stordal, F. 1997. High latitude springtime photochemisty part 1: NO_x, PAN, and ozone relationships. *J. Atmos. Chemistry*, in press.

Bottenheim, J. W., Barrie, L. A., Atlas, E., Heidt, L. E., Niki, H., Rasmussen, R. A. and Shepson, P. B. 1990. Depletion of lower tropospheric ozone during arctic spring. The Polar Sunrise Experiment 1988. *J. Geophys. Res.* **95**, 18, 555–18, 568.

Curry, J. A. and Radke, L. F., 1993. Possible role of ice crystals in ozone destruction of the lower arctic atmosphere. *Atmos. Environ.* **27**, 2873–2879.

Fan, S.-M. and Jacob, D. 1992. Surface ozone depletion in arctic spring sustained by bromine reactions on aerosols. *Nature* **359**, 522–524.

Finlayson-Pitts, B. J., Livingston, F. E. and Berko, H. N. 1990. Ozone destruction and bromine photochemistry at ground level in the arctic spring. *Nature* **343**, 622–625.

Hansen-Bauer, I., Kristensen Solås, M. and Steffensen, E. L. 1990. The climate of Spitsbergen. *DNMI-Rapport 39/90 Klima*, Det Norske Meteorologiske Institutt, Oslo.

Hausmann, M. and Platt, U. 1994. Spectroscopic measurement of bromine oxide and ozone in the high Arctic during Polar Sunrise Experiment 1992. *J. Geophys. Res.* **99**, 25, 399–25, 414.

Hopper, J. F., Peters, B., Yokouchi, Y., Niki, H., Jobson, B. T., Shepson, P. B. and Muthuramu, K. 1994. Chemical and meteorological observations at ice camp SWAN during Polar Sunrise Experiment 1992. *J. Geophys. Res.* **99**, 25, 489–25, 498.

Hopper, J. F. and W. Hart, 1994. Meteorological aspects of the 1992 Polar Sunrise Experiment. *J. Geophys. Res.* **99**, 25, 315–25, 329.

Jobson, B. T., Niki, H., Yokouchi, Y., Bottenheim, J., Hopper, F. and Leaitch, R. 1994. Measurements of C2-C6 hydrocarbons during the Polar Sunrise 1992 Experiment: Evidence for Cl atom and Br atom chemistry. *J. Geophys. Res.* **99**, 25, 355–25, 368.

Kley, D. and McFarland, M. 1980. Chemiluminescence detector for NO and NO_2. *Atmos. Technology* **12**, 63–69.

Le Bras, G. and Platt, U. 1995. A possible mechanism for combined chlorine and bromine catalyzed destruction of tropospheric ozone in the Arctic. *Geophys. Res. Lett.* **22**, 599–602.

Lin, X., Trainer, M. and Liu, S. C. 1988. On the nonlin-

earity of the tropospheric ozone production. *J. Geophys. Res.* **93**, 15, 879–15, 888.

Liu, S. C., Trainer, M., Fehsenfeld, F. C., Parrish, D. D. Williams, E. J., Fahey, D. W., Hübler, G. and Murphy, P. C. 1987. Ozone production in the rural troposphere and the implications for regional and global ozone distributions. *J. Geophys. Res.*, **92**, 4191–4207.

McConnell, J. C., Henderson, G. S., Barrie, L., Bottenheim, J., Niki, H., Langford, C H. and Templeton, E. M. J. 1992. Photochemical bromine production implicated in arctic boundary layer ozone depletion. *Nature* **355**, 150–152.

McGrath, R. 1989. Trajectory models and their use in the Irish Meteorological Service. *Internal Memorandum No. **112/89***, Irish Meteorological Service, Glasnevin Hill, Dublin, 12.

Miller, J. C. and Miller, J. N. 1984. Nonparametric regression methods. *Statistics for analytical chemistry*, New York: Wiley, 132–134.

Solberg, S., Schmidbauer, N., Semb, A., Stordal, F. and Hov, Ø. 1996a. Boundary-layer ozone depletion as seen in the Norwegian Arctic in spring. *J. Atmos. Chem.*, **23**, 301–332.

Solberg, S., Dye, C., Schmidbauer, N., Herzog, A. and Gehrig, R. 1996b. Carbonyls and nonmethane hydrocarbons at rural sites from the Mediterranean to the Arctic. *J. Atmos. Chem.* **25**, 33–66.

Staebler, R. M., Den Hartog, G., Georgi, B., Landsberger S. and Düsterdiek, T. 1994. Aerosol size distributions in Arctic haze during the Polar Sunrise Experiment 1992. *J. Geophys. Res.*, **99**, 25, 429–25, 438.

Sturges, W. T., Schnell, R. C., Landsberger, S., Oltmans, S. J., Harris, J. M. and Li, S.-M. 1993. Chemical and meteorological influences on surface ozone destruction at Barrow, Alaska, during Spring 1989. *Atmos. Environ.* **27A**, 2851–2863.